Analysis of Angular Dependent Resistance Measurements on IrMn-Based Spin Valves Using a Finite Pinning Model

Chih-Ling Lee, Shaoyan Chu, James A. Bain, and Michael E. McHenry

***Abstract*—The magnetoresistance of IrMn based spin valve sheet films has been measured as a function of applied field orientation and temperature. Analysis of these angular resolved results allows the separation of the magnetic response of each ferromagnetic layer in the structure. Specifically, the data are fitted to a model of magnetoresistive response that accounts for giant magnetoresistance (GMR) effects between the two layers and anisotropic magnetoresistance (AMR) effects within each layer. Both the pinned and free ferromagnetic layers are assumed to be single domains. Additionally, the free layer is assumed to follow the applied field, while the pinned layer follows the vector sum of the applied field and the pinning field. From the fitting results, several parameters are separated quantitatively, including the resistance change associated with GMR and AMR effects, the misalignment angle for the pinned layer, the angular excursion of the pinned layer under external field, the average current direction and the thermal coefficient of resistance. This analysis can support the design of spin valve readers, especially when extended to the determination of the canting angle of the pinned direction for patterned devices.**

***Index Terms*—AMR, angular dependent measurement, anisotropy magnetoresistance, canting angle, giant magnetoresistance (GMR), IrMn, magnetic recording heads, memory device, spin valve.**

I. Introduction

FOR high-density recording, an important issue is to control the magnetization rotation of the sensing layer such that it moves stably during the sensing of the magnetic field. This is especially true when the device is patterned into fine dimensions. A primary task in controlling magnetization rotation is to be able to measure it in both the quiescent and driven states. This work develops a technique suitable for this task.

In this work, the giant magnetoresistance (GMR) effect is assumed proportional to the cosine of the angle between the free layer and the pinned layer while the AMR effect is assumed proportional to the cosine squared of the angle between the net magnetization and the current direction. A spin valve sheet films resistance has been measured as a function of a rotating applied field. By using a model to fit the experimental results, all physical parameters of the system can be quantitatively determined. Several individual experiments had been designed to examine these fitting parameters, and the supporting experimental results agree with the fitting results. This model is developed below.

Manuscript received February 1, 2002; revised May 22, 2002. This work was supported in part by the National Science Foundation under Grant ECD-8907068.

The authors are with the Department of Materials Science and Engineering, Carnegie Mellon University, PA 15213 USA (e-mail: zlee@andrew.cmu.edu; sc79@andrew.cmu.edu; mm7g@andrew.cmu.edu; jbain@ece.cmu.edu).

Digital Object Identifier 10.1109/TMAG.2002.803125.

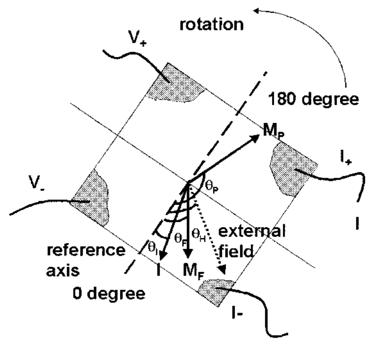

Fig. 1. Four point measurement for as-deposited IrMn spin valve. The sample is rotated under a fixed external field.

II. Experiment

The structure of the IrMn spin valves studied in this work was glass/Ta 26 Å/NiFe 47 Å/CoFe 21 Å/Cu 24 Å/CoFe 13 Å/NiFe 22 Å/IrMn 124 Å/Ta26 Å. They were prepared by dc magnetron sputtering. During deposition, a uniaxial magnetic field of 30 Oe was applied in a direction defining the sample's reference axis. The sheet resistance of the spin valves was 20 Ω/square. The angular dependent resistance was measured by a Physical Property Measurement System (PPMS) Model 6000 made by Quantum Design Co. The samples were cut into 5 mm × 5 mm squares, loaded in the PPMS and oriented relative to the instrument as shown in Fig. 1. The magnetic field was fixed while the sample was rotated within this field. The coordinates given in Fig. 1 are relative to the sample reference axis. As the film was rotated, the free layer remained largely parallel to the external field. The resistance was measured by the four point contact method. The contact region was sputtered Au with a thickness of 150 nm.

III. Finite Pinning Model of Magnetoresistance

The model of spin valve resistance used in this work was as follows. The total resistance, R, of a spin valve can be expressed as a combination of GMR and AMR effects according to [1], [2]

$$R = R_0 + \frac{1}{2}\,\Delta R_{GMR}^{\max}\,[1-\cos(\theta_F-\theta_P)] + \Delta R_{AMR}^{\max} \cdot \left[\alpha\cos^2(\theta_F-\theta_I) + (1-\alpha)\cos^2(\theta_P-\theta_I)\right] \quad (1)$$

where R_0 (Ω) is the reference resistance of the film, which refers to the state where the free layer and pinned layer are aligned to each other and they are also perpendicular to the current direction. $\Delta R_{GMR}^{\max}$ (Ω) is the maximum change in resistance due to the GMR effect and $\Delta R_{AMR}^{\max}$ (Ω) is the maximum change in resistance due to the AMR effect. A scaling factor, α, defined as the fraction of total AMR contribution from the free layer, is used to combine the AMR effect for both the pinned and free layer. The relative angles of θ_F, θ_P and θ_I are shown in Fig. 1. The electrical transport properties of multilayers have been extensively investigated with regard to both interfacial scattering and bulk scattering [3]. In this model, the GMR effect is considered to be dominated by interfacial scattering and the AMR effect is taken to be bulk scattering dominated. Experimentally, we measure R as a function of the applied field angle, θ_H. In all cases, single domain behavior is assumed for the pinned and free layers. In this work, the free layer is assumed to be in the same direction as the external field because the external field is much larger than the total anisotropy field of the free layer. In other words, θ_F is set equal to θ_H (see Fig. 1), i.e., $\theta_F(\theta_H) = \theta_H$. The pinned layer is assumed to be oriented in a certain direction, defined by θ_{P0}. In order to capture the finite nature of the pinning field, the torque on the pinned layer is calculated through the total energy of the pinned layer

$$E = -M_P H_{appl} \cos(\theta_P - \theta_H) - M_P H_{ex} \cos(\theta_P - \theta_{P0}) \quad (2)$$

where M_P is the magnetization of the pinned layer, H_{appl} is the magnitude of the applied field, H_{ex} is the magnitude of the exchange pinning field, θ_{P0} is the direction in which this exchange field is directed relative to the reference axis, and θ_H and θ_P are still as defined in Fig. 1. This yields a torque on the pinned layer, through–$(\partial E/\partial \theta_P)$.

Setting this torque equal to zero and simplifying yields the following expression:

$$\theta_P(\theta_H) = \tan^{-1}\left(\frac{\sin\theta_{P0} + \gamma \sin\theta_H}{\cos\theta_{P0} + \gamma\cos\theta_H}\right) \quad (3)$$

where $\gamma = H_{appl}/H_{ex}$, the applied field normalized by the exchange field.

This relationship is the essence of the finite pinning model, and allows the plot of R versus θ_H to be fitted using the following parameters: R_0, $\Delta R_{GMR}^{\max}$, $\Delta R_{AMR}^{\max}$, α, θ_{P0}, θ_I and γ. Since γ is a function of H_{ex}, the temperature dependence of H_{ex} has been implicitly included in the γ term.

IV. Results

Typical angular dependent measurement results at 290 K are shown in Fig. 2. In the figure, resistance is plotted versus θ_H for different applied fields. For θ_H values near 0° or 360°, a high resistance state is shown. This indicates the pinned layer and the free layer are anti-parallel to each other for this value of θ_H. Low resistance is seen in the mid angle range, indicating the pinned layer and the free layer are parallel to each other near $\theta_H = 180°$. At low field, the periodicity of the resistance response is 360°, which corresponds to a cosine behavior and indicates the GMR effect dominates the resistance response. When the external field increases above 300 Oe, the resistance response

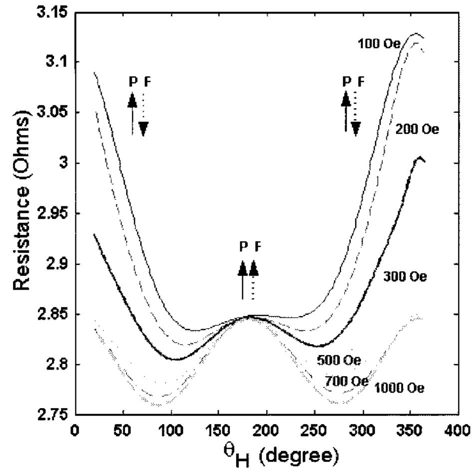

Fig. 2. Resistance versus θ_H at 290 K under different external fields.

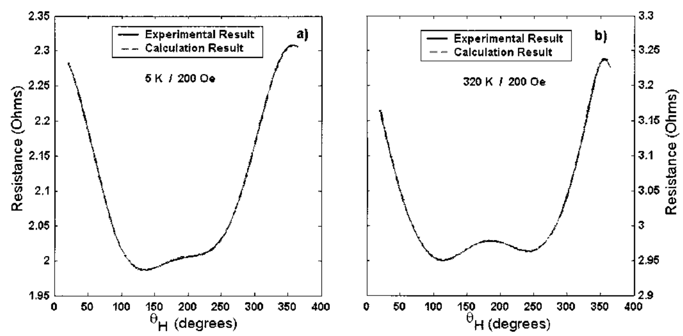

Fig. 3. Typical fitting results for the pinning model. The (a) low temperature data and (b) the high temperature fitting are perfectly fitted with the model.

periodicity changes from 360° to 180°, which corresponds to a cosine squared behavior and the AMR effect being dominant.

From these results, it can be deduced that the exchange field is between 200 Oe and 300 Oe. When the external field increases above 300 Oe the pinned layer is activated and the exchange coupling no longer constrains the pinned layer. Consequently, the GMR effect is diminished and the AMR effect dominates the resistance response.

The results of applying the finite pinning model to the $R(\theta_H)$ plots for the spin valve structure described in the experimental section of this work are shown in Fig. 3. Fig. 3(a) shows R for a field magnitude of 200 Oe, at 5 K and Fig. 3(b) shows the results at the same field but at a temperature of 320 K. Both low temperature and high temperature data can be fitted with the finite pinning model perfectly.

The samples in this study were fitted with the finite pinning model for a range of temperatures from 5 K to 320 K. The results of fitting the angular dependent resistance to this model are shown in Fig. 4. Initial inspection of these plots reveals a few expected trends. The reference resistance, R_0, increases with temperature, as does γ, the ratio of the applied field, H_{appl}, to the exchange pinning field, H_{ex}. The GMR ($\Delta R_{GMR}^{\max}$) and AMR ($\Delta R_{AMR}^{\max}$) coefficients decrease slightly with temperature. The fraction of the free layer contribution to the AMR, given by α, is, as expected for these films, around 60%, and the two angles, θ_{P0} and θ_I are consistent with experiment. More detailed discussion of these results is provided below.

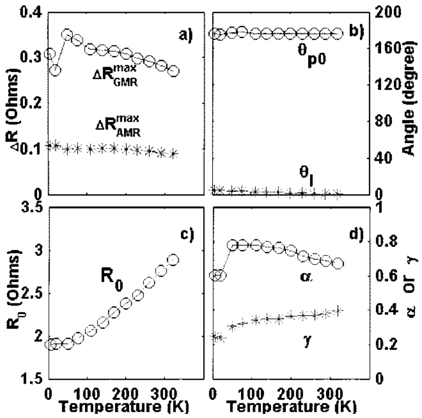

Fig. 4. Fitting parameters plotted as function of temperature under an external field of 100 Oe.

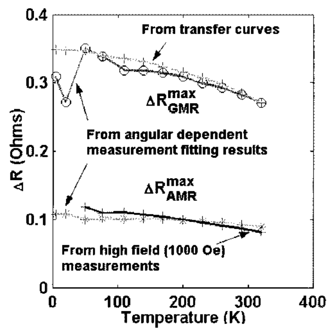

Fig. 5. Fitting results of ΔR versus temperature compared with the experimental results from transfer curves (GMR) and high field (1000 Oe) results (AMR).

V. Discussion

The fitting results for $\Delta R^{\max}_{GMR}$ and $\Delta R^{\max}_{AMR}$, in Fig. 4(a), are compared with the corroborating experimental results in Fig. 5. In this figure, the fitting results for $\Delta R^{\max}_{GMR}$ are compared to the difference between the high resistance state and the low resistance state obtained from the standard MR transfer curves. Also in Fig. 4, the experimental results for $\Delta R^{\max}_{AMR}$ are compared with the difference between the high resistance state and the low resistance state from high field angular dependent data. This high field data was collected at an applied field of 1000 Oe. As shown in Fig. 2 this is sufficient to smoothly rotate the pinned layer. The fitting results in both of these cases are very close in value to the corroborating experimental values, indicating the validity of the fitting procedure.

From the fitting results above several features can be noted. Firstly, the resistance change attributed to the GMR effect ($\Delta R^{\max}_{GMR}$) and the AMR effect ($\Delta R^{\max}_{AMR}$) decrease modestly with increasing temperature, as expected. These values go from 0.31 to 0.27 Ω (GMR) and from 0.11 to 0.09 Ω (AMR) over the range of temperatures examined (5 K to 320 K). The reference resistance, R_0, also increased with temperature as expected, yielding a thermal coefficient of resistance (TCR) [4] of 0.18%/°C.

The GMR% (computed as $\Delta R^{\max}_{GMR}/R_{\min}$) and AMR% (computed as $\Delta R^{\max}_{AMR}/R_{\min}$) dropped from 17.5% to 9.2% and from 5% to 3%, respectively, over the same temperature range. $R_{\min}$ is the minimum resistance measured as a function of angle. Fig. 4(b) indicates a pinned layer misalignment of approximately 5° away from the reference axis. The average current direction, θ_I, is 2° from the reference axis for both cases. These results agree with the direction of applied current for the four point measurement as shown in Fig. 1. It should be noted that this agreement suggests that this method could be used to identify canting of the pinned layer in patterned devices

The α term, which is the fraction of the total AMR effect coming from the free layer is shown in Fig. 4(d). These results show that the free layer has a higher contribution to the AMR effect than the pinned layer. This is likely to be related to the thickness of the free and pinned layer given the assumption of bulk scattering for the AMR effect, since the thickness of the free and the pinned layer is about 2 : 1.

The γ term, which is the ratio of the applied field over the exchange field, is also shown in Fig. 4(d). When the temperature is raised, γ increases. This corresponds to the exchange field decreasing as temperature increases. Furthermore, the maximum excursion angle at 320 K for a 200 Oe external field is ±42° for the pinned layer, which is calculated by (3), as shown in Fig. 6.

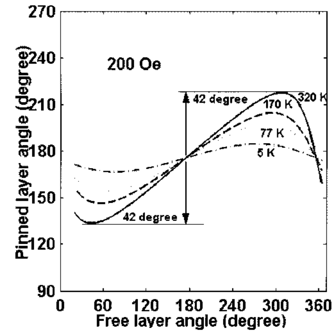

Fig. 6. Pinned layer maximum rotation angle at different temperatures under a 200 Oe external field.

VI. Conclusion

The resistance of IrMn spin valves has been measured as a function of applied field angle with varying temperature and field magnitude. By using the model in this paper, a set of fitting parameters describing the resistance, magnetoresistance, layer orientations and exchange fields have been quantitatively separated. These fitting parameters have also been confirmed by separate experiments. Using this approach, the misalignment of the pinned direction has been identified to be about 5° away from the reference axis, for a sheet film. This analysis method and experiment can support the design of magnetic recording heads or memory devices.

References

[1] B. H. Miller, E. Y. Chen, and E. D. Dahlberg, *J. Appl. Phys.*, vol. 73, no. 10, p. 6384, 1993.

[2] T. G. S. M. Rijks and R. Coehoorn *et al.*, *J. Appl. Phys.*, vol. 76, no. 2, p. 1092, 1994.

[3] B. A. Gurney and V. S. Speriosu *et al.*, *Phys. Rev. Lett.*, vol. 71, no. 24, p. 4023, 1993.

[4] B. Dieny *et al.*, *Phys. Rev. B*, vol. 45, no. 2, p. 806, 1992.